Measurement of the Thermal Expansion of Pure Water in the Temperature Range 0°C-85°C

1990 Metrologia 27 165

(http://iopscience.iop.org/0026-1394/27/4/001)

Metrologia 27, 165–171 (1990)

metrologia

Measurement of the Thermal Expansion of Pure Water in the Temperature Range 0 °C–85 °C

M. Takenaka and R. Masui

National Research Laboratory of Metrology, 1-1-4, Umezono, Tsukuba, Ibaraki 305, Japan

Received: March 5, 1990 and in revised form May 28, 1990

Abstract

The thermal expansion of pure water having natural isotopic abundance was determined by the dilatometric method in a temperature range from 0 to 85 °C and under a pressure of 101 325 Pa. The following equation was obtained:

$$\varrho(t)/\varrho_{\max} = 1 - \frac{(t-3{,}98152)^2\,(t+396{,}18534)\,(t+32{,}28853)}{609\,628{,}6(t+83{,}12333)\,(t+30{,}24455)},$$

where $\varrho(t)$ is the density of water at temperature t, which is expressed in terms of the ITS-90, and $\varrho_{\max}$ the maximum density. The density ratio which the above equation gives is estimated to have an uncertainty of approximately 1×10^{-6}.

1. Introduction

Water has been used in a number of fields as one of the standard materials of density. The most accurate values currently in use are based substantially on two sets of thermal expansion measurements made at the Bureau International des Poids et Mesures (BIPM, 0–41 °C) [1] and the Physikalisch-Technische Reichsanstalt (PTR, 0–42 °C) [2], and the absolute measurement made at BIPM [3]. However, the maximum difference between the two thermal expansion measurements amounts to 8 ppm in density near 40 °C, and the relationship between the temperature scale used at the time of measurement and the present scale, ITS-90, is not known with sufficient accuracy. An extensive account of the present status of the density of water is given in references [4, 5]. These problems can be solved satisfactorily only by making new measurements [6].

Here, we describe our new measurement of the thermal expansion of pure water, which is a measurement of the ratio $\varrho(t)/\varrho_{\max}$ as a function of temperature, where $\varrho(t)$ is the density at t °C and 101 325 Pa, and $\varrho_{\max}$ the maximum density at 101 325 Pa. The method we used is a dilatometric one, and the temperature range covered is 0–85 °C. The dilatometer consists of a 100 cm^3 water cell, a capillary tube with a mercury bulb on one end, and a weighing bottle. The water cell is placed in a thermostat, and the capillary connected to it penetrates the thermostat wall and opens to the atmosphere outside the thermostat. Expansion of water causes the mercury, which is put in the cell together with water, to be pushed through the capillary and to come out of the end which is outside the thermostat. The mercury is received in the weighing bottle, and the change in mass of the bottle is measured by a balance. The dilatometer is so designed that it can be disassembled into parts and the thermal expansion of the cell itself can be measured directly by optical interferometry.

2. Experimental

2.1. Sample Water

The water samples we used have a natural isotopic composition, and since it has been established that the thermal expansion is not affected seriously by small variations of the isotopic content [4, 5], we exclusively used purified tap water taken from an outlet of NRLM in this study. The isotopic composition of our purified tap water, as measured in another experiment [7], is approximately $\delta^{18}O = -4{,}5‰$, $\delta D = -35‰$, and the corresponding deviation in absolute density from Standard Mean Ocean Water is $-1{,}6$ ppm.

The purification was made by a process including a reverse osmosis, adsorption by activated carbon, ion exchange and a final filtration by a filter having, 0,22 μm rated pore size. The processed water still contained air which was removed by evacuating the water while stirring. The air bubbles ceased to rise after half an hour, and we continued the evacuation for another hour. A chemical analysis using the Winkler method showed that the oxygen content in the degassed sample was less than 1% of saturation. The concentration of nitrogen was not mea-

sured, but we assumed that nitrogen was also removed by a similar amount. Since the density change due to the dissolved air at saturation is known to be 4 ppm at maximum [8], the effect of residual air in our samples should be negligibly small. The purity of water thus processed has also been checked by density comparison with water prepared by careful distillation of sea water [7]. The comparison with a resolution of 0,1 ppm showed that the densities of two purified water samples coincided exactly after the isotopic correction was made. Considering that the sources and the purification processes of the two samples are completely different, it is unlikely that the coincidence can be interpreted by an identity of the impurity effects on the two samples. Hence we conclude that the density errors due to the impurities remaining in both samples were less than 0,1 ppm.

2.2. *Dilatometer*

The dilatometer is shown schematically in Fig. 1. It comprises four major parts, a water cell, a capillary, a top plate and a weighing bottle. These parts are made of fused quartz. The water cell is a cylindrical vessel, 4 cm in o.d. and 10 cm long, with a capacity of about 100 cm^3. The cell has a cylindrical projection on each end plate and the projection has a stainless steel ring around it, as shown in Fig. 1 A. The side of the ring is threaded to secure a metal cap which holds the top plate on the top end of the cell, and the flanged end of the capillary on the bottom end of the cell, so that the three parts of the dilatometer can thus be assembled. The coupling device was designed to minimize the volume change of the cell due to elastic deformation when the end projections are squeezed with screws for mounting the rings.

The capillary is 0,7 mm in i.d. and has a mercury bulb close to the flanged end. The bulb and the capillary are filled with mercury. The other end of the capillary is cut at a position which comes to the same height as that of the center of the bulb when the assembly is supported upright. This cancels most of the pressure caused by the mercury column in the capillary. The top plate is circular and seals off the cell. The contact on each end of the cell is sealed by a trace of Apiezon grease. As the temperature is raised and the water pushes the mercury through the capillary, the excess mercury comes out and is received by the weighing bottle.

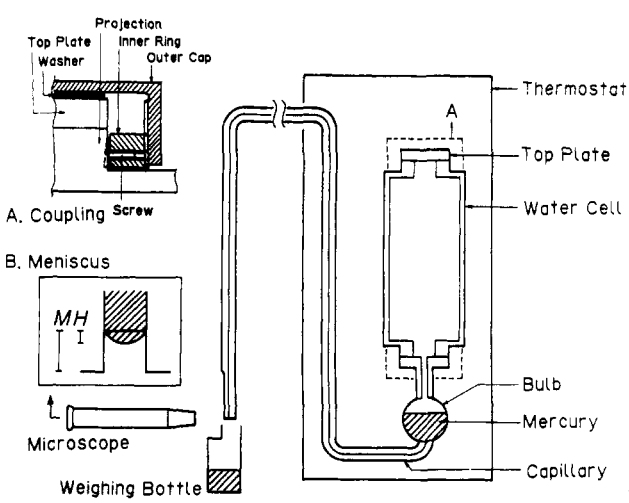

Fig. 1. Dilatometer. **A** Mechanism for coupling the top plate and the flange to the ends of the water cell. **B** View through the microscope of the mercury head

For cleaning, the water cells were removed from the metal fittings. All the glass parts were treated in a chromic acid mixture for several days, rinsed with pure water and dried at 70 °C in a drying chamber. The parts of the dilatometer were then assembled, except the top plate, and about 5 cm^3 of mercury was put into the bulb from the top opening of the cell. The mass of the assembly was measured. Degassed sample water was then introduced from the same opening under vacuum. After the cell was closed by means of the top plate, the mass of the dilatometer was measured again to obtain the mass of sample water filling the cell.

When the dilatometer was filled, we made sure that no air bubbles were left in the dilatometer. In particular, bubbles trapped between the mercury and glass wall do not dissolve, and cause significant errors. A small amount of mercury was then put into the weighing bottle and, after the tip of the capillary had been dipped in the mercury, a connection was made between the mercury in the capillary and the mercury in the bottle by warming the water cell.

The dilatometer was then secured on a support (not shown) and the whole assembly was placed in the thermostat bath. A capsule-type platinum resistance thermometer enclosed in a brass tube was mounted near the cell for measurement of the temperature of the sample water. The dilatometer in the bath was first heated to the highest temperature of measurement (85 °C) and kept for a few days at that temperature in order to anneal the grease layers between the contact surfaces. This kept the total capacity of the dilatometer stable during a run of measurement.

The measurement procedure is as follows. The thermostat temperature is first lowered to 0 °C, the starting point, and measurements are made as the temperature is raised stepwise, with the interval depending upon the curvature of the expansion curve. Because the coefficient of thermal expansion of water is negative between 0 °C and 4 °C, reconnections of mercury thread are made by heating the cell up to about 8 °C and then cooling it again to the next temperature until the measurement temperature exceeds 4 °C. Every time a temperature equilibrium is attained, the mass of the weighing bottle is measured using an electronic balance which has been calibrated to an accuracy of 10 μg. The air buoyancy correction is made by calculating the density of air from the measured values of atmospheric pressure, temperature and relative humidity using the formula of CIPM81 [9].

Every time the weighing bottle is removed from the capillary for weighing, the continuity of the mercury thread is broken. Since the position where the mercury thread is cut is not strictly reproducible, the mass of the mercury in the weighing bottle must be corrected for the variation in the position of the mercury head in the capil-

lary. Accordingly, the position of the mercury head (M) is measured by a traveling microscope. The mercury head in the capillary forms a convex meniscus as shown in Fig. 1 B. The joint effect of the meniscus and the surface tension causes a pressure rise inside the dilatometer. For estimation of this pressure rise, the height of the bulge of the mercury head (H) is also measured by the microscope and the radius of curvature (r) is calculated. The pressure rise (ΔP) due to the surface tension (γ) is given by $\Delta P = 2\gamma/r$, if a spherical form is assumed for the mercury head.

Since the capillary is open to the atmosphere, the water sample, mercury and the cell are all subjected to variations of the total pressure. There are two different kinds of pressure effect in this dilatometer. One is pressure variation which takes place equally both inside and outside of the dilatometer. The variation of the atmospheric pressure is of this kind. The other kind causes a pressure change inside the dilatometer only, resulting in a pressure difference between the inside and the outside of the dilatometer. The surface tension described above and the mercury column in the capillary cause this kind of effect. The first kind of effect causes an expansion or contraction of water and mercury, and the second kind causes an elastic inflation or deflation of the cell in addition to the volume change of water and mercury.

The change of the density of water and mercury due to pressure change was calculated from the literature values of compressibilities [5, 10]. The elastic expansivity of the dilatometer cell was determined experimentally by applying known pressure differences between the inside and outside of the cell.

The pressure due to the mercury column in the capillary changes as the height of the mercury surface in the bulb changes as a function of the amount of mercury left in the bulb, i.e., as a function of temperature. The relationship between the height of the mercury surface in the bulb and the volume of the mercury remaining in the bulb has been calibrated.

2.3. *Thermostat*

For control of the temperature of the dilatometer, a new thermostat was designed and built for this measurement.

The thermal expansivity of water increases rapidly as the temperature rises and at 85 °C, the highest temperature of this study, a variation of 1 mK causes a change of 0,7 ppm in density. In order to meet the accuracy requirement of the measurement, a thermostat whose temperature stability is better than ±0,2 mK over the entire temperature range between 0 °C and 85 °C has been developed.

Figure 2 illustrates the setup of the thermostat. The water bath is made of an aluminum cylinder of 16 cm o.d. and 14 cm i.d. A film heater and a copper cooling tube are wound on the outside surface of the cylinder for uniform heating and cooling. A thermistor is buried in the aluminum wall as the sensor for the control system. The bath cylinder is surrounded by a thermal insulator, of thickness 10 cm, which is made of urethane foam and rock wool. Water in the bath is stirred by a propeller which is

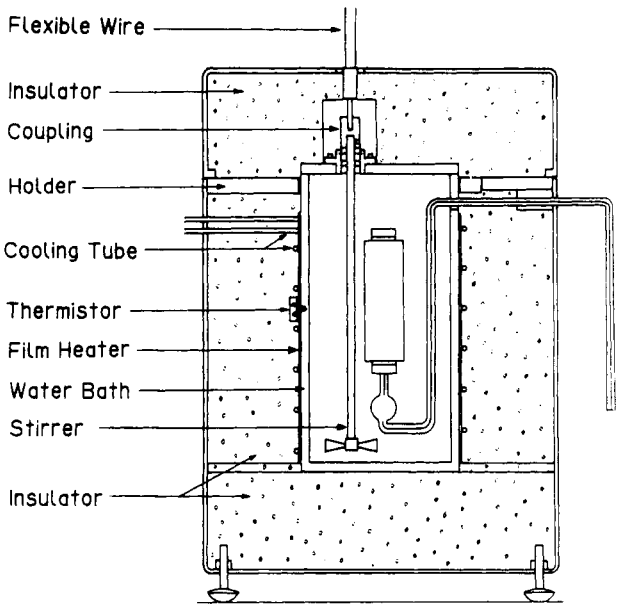

Fig. 2. Thermostat with dilatometer placed in it

driven from outside through a flexible rod to avoid vibration. An a.c. bridge incorporating the thermistor is used to detect temperature. The output signal from the bridge is amplified by a lock-in and supplied to a controller to generate a control voltage. This, in turn is sent to a programmable power supply for control of the heater current.

The scatter and drift of the temperature were ±0,1 mK in the range below 50 °C and ±0,2 mK at 85 °C. The maximum temperature difference in the bath was 1 mK or less at all temperatures. The thermostat was placed in an underground laboratory to improve the temperature environment.

2.4. *Temperature Measurement*

The temperature of the sample water was measured by a capsule-type platinum resistance thermometer placed close to the water cell. The thermometer had been calibrated at the triple point of water and the triple point of indium in the Thermometry Section of NRLM (the value of the coefficient a was determined according to 3.3.2.4 in the ITS-90 [11]). The R (0,01 °C) was checked in a triple-point cell before and after each series of measurements to confirm the absence of an accidental change of the resistance. An increase in R (0,01 °C), which corresponds to 3 mK in temperature, was observed during the one-year period between the third-series and the fourth-series measurements, and the thermometer was recalibrated before resumption of the measurement. The resistance ratio $R(t)//R(0{,}01\ °C)$ was converted to temperature according to the ITS-90 [11]. The temperature of the bath was also monitored by a quartz thermometer, and the readings were recorded to check the temperature stability. The small amount of mercury contained in the part of the capillary which penetrates the thermostat wall is in a temperature gradient. In order to correct for the thermal

expansion of mercury in the gradient, four small holes were bored at 40 mm intervals in this part of the capillary, and four thermocouples were mounted.

2.5. *Thermal Expansion of the Fused Quartz Cells*

A knowledge of the thermal expansion of the cell itself is necessary for the dilatometry. Since the coefficients of thermal expansion of fused quartz differ from sample to sample, due probably to the impurities contained and to differences in thermal history [12], use of literature values is not sufficient when an accuracy of 1 ppm is required of the density measured. This means that thermal expansion must be measured directly on the very dilatometers used in the measurement. We used optical interferometry, and Fig. 3 shows the principle of the measurement.

The water cell is so designed that it is separable from the remaining parts and can be used as a spacer in a Fizeau interferometer. The face of each end of the cell is polished flat to allow optical contact with a flat mirror. The mirrors used are coated with circular reflecting films with diameters of 10 mm and a reflectivity of 0,8. The reflecting surfaces of the two mirrors form an angle of about $7{,}3 \times 10^{-5}$ rad, so that two or three interference fringes are always observable. A stabilized He-Ne laser ($\lambda = 633$ nm) is used as the light source. The light beam is expanded to 10 mm in diameter and introduced into the interferometer. The beams coming back are reflected by a beam splitter. After being condensed to a point, spurious reflections are removed by a pinhole. Fringes are photographed by placing a photographic film on the observation plane. One of the mirrors carries two marks of triangular shape which give the reference points for reading fringe positions. The finesse of the fringes in this multiple beam interferometer is 15. The fringes observed are neither straight nor at regular intervals because of slight undulations of the mirror surfaces. This effect is corrected by approximating the undulation with a quadratic curve.

The interferometer was set in a vacuum chamber to eliminate the effect of the refractive index of air. For evacuation, the space inside the cell was connected with the outside through a hole provided on the mirror plate. The pressure of the residual air, as measured by a Pirani gauge, ranged from 2,5 Pa to 4,5 Pa depending on temperature. The vacuum chamber was temperature controlled, and three copper-constantan thermocouples were mounted on the cell to monitor the temperature gradient.

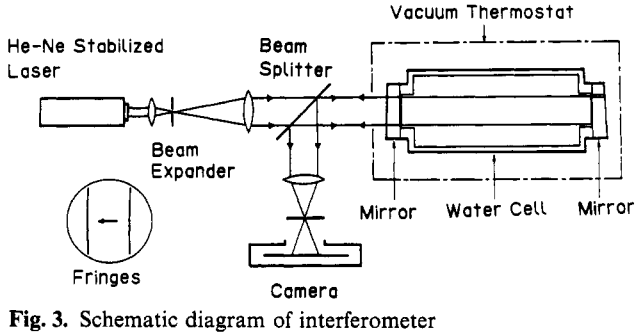

Fig. 3. Schematic diagram of interferometer

The temperature difference between the two ends of the cell amounted to 0,2 K at the highest measurement temperature (85 °C). The gradients in the other two directions were negligible. The temperature of the cell was measured with a capsule-type platinum resistance thermometer placed close to the cell. The optical axis of the interferometer was first aligned at room temperature, but the axis went out of alignment as the temperature was changed because of non-uniform thermal expansion of various components of the thermostat and the interferometer. The interferometer was realigned every time such a misalignment was detected.

The fringes were observed at 11 temperatures distributed at equal intervals between 0 °C and 85 °C. The relative positions of the fringes with respect to the reference marks were analyzed by magnifying the photographic image on a viewer screen. The change in length ΔL of the water cell is calculated by the following equation:

$$\Delta L = (\Delta N + \Delta\varepsilon)\,\lambda/2 \tag{1}$$

where ΔN is the change in the integral part, $\Delta\varepsilon$ the change in the fractional part of the order of interference, and λ the wavelength of the He-Ne laser. The ΔN was counted by observing the movement of the fringes as the temperature was changed. The $\Delta\varepsilon$ was calculated from the relative positions of fringes with respect to the reference marks. The initial value of the cell length was measured by a mechanical contact micrometer. The relative change of the cell length $\Delta L/L$ was thus obtained as a function of temperature. The volume expansion was calculated from the linear expansion assuming the isotropy of the material.

For cells No. 1 and 2, measurements were made at 14 temperatures each, and for cell No. 3, they were made at 15 temperatures. The data for each cell were fitted to a third-order polynomial. The parameters are listed in Table 1 together with the standard deviations of the fittings.

The thermal expansion of the mercury bulb and the capillary was not measured but was assumed to be equal to the thermal expansion of the water cell.

2.6. *Treatment of Data*

The measured data were treated in the following way to obtain the relative density as a function of temperature. For normalization of the data, the measured values of the mass of the weighing bottle were corrected to the values they would have taken had the sample water been at a pressure of 101 325 Pa, the pressures inside and outside of the dilatometer been equal, and the capillary been filled up with mercury exactly to the end. The mass of the weighing bottle was also corrected for the temperature distribution along the capillary.

The corrected mass of the weighing bottle at each temperature is related to the volume change of the sample water by the following equation:

$$\begin{aligned} M_M(t) - M_M(t_{ref}) = {} & \{V_D(t_{ref}) - V_W(t_{ref})\}\,\varrho_M(t_{ref}) \\ & - \{V_D(t) - V_W(t_{ref}) - \Delta V_W(t)\}\,\varrho_M(t) \end{aligned} \tag{2}$$

where $M_M(t)$ and $M_M(t_{ref})$ are, respectively, the mass of the mercury bottle at t and at the reference temperature t_{ref} which is chosen close to 4 °C; $V_D(t_{ref})$ and $V_D(t)$ are the internal volumes of the dilatometer at temperatures t_{ref} and t, respectively. The $\varrho_M(t_{ref})$ and $\varrho_M(t)$ are the densities of mercury, at their respective temperatures, given in the literature [13]. The difference between the present temperature scale and the IPTS-48 used in the literature has been taken into account. The quantity $V_W(t_{ref})$ is the volume of the sample water at the reference temperature. The $\Delta V_W(t)$ is the volume change of the sample water $(V_W(t) - V_W(t_{ref}))$, which is the quantity to be calculated from the equation.

The volume of the water cell at the reference temperature, $V_D(t_{ref})$, was determined by weighing the cell filled with water, and the volume of the capillary (plus bulb) was determined by weighing it while it was filled with mercury. The $V_D(t)$ was obtained from the knowledge of $V_D(t_{ref})$ and the thermal expansion of the cell measured by optical interferometry.

The volume change calculated in the above is used to calculate the density ratio $\varrho(t)/\varrho_{max}$, which is given by

$$\varrho(t)/\varrho_{max} = M_W / \{[\varrho_{max}/\varrho(t_{ref})]\, M_W + \varrho_{max}\, \Delta V_W(t)\}\,, \qquad (3)$$

Table 1. Fittings of linear thermal expansion of water cells to the third polynomial

Cell No.	$[L(t)-L(0)]/L(0) = A\,t + B\,t^2 + C\,t^3$			Standard deviation of fitting
	A	B	C	
1	$3{,}9185 \times 10^{-7}$	$1{,}3178 \times 10^{-9}$	$-2{,}9128 \times 10^{-12}$	3×10^{-8}
2	$3{,}9491 \times 10^{-7}$	$1{,}4374 \times 10^{-9}$	$-3{,}8549 \times 10^{-12}$	2×10^{-8}
3	$3{,}9102 \times 10^{-7}$	$1{,}4646 \times 10^{-9}$	$-4{,}1148 \times 10^{-12}$	2×10^{-8}

where M_W is the mass of sample water and $\varrho(t_{ref})$ the density of water at the reference temperature. According to (3), the density ratio is, in principle, calculated only if independent knowledge of ϱ_{max} and $\varrho(t_{ref})$ is available. However, the relative density is less affected by the uncertainty included in ϱ_{max}. Since t_{ref} is close to 4 °C, $\varrho_{max}/\varrho(t_{ref})$ is substantially equal to unity, irrespective of the possible measurement uncertainty involved in the absolute density, and $\Delta V_W(t)$ is a relatively small quantity. We used $\varrho_{max} = 999{,}9734$ kg/m^3 assuming that the ϱ_{max} for Standard Mean Ocean Water is 999,975 kg/m^3, and the correction due to the difference in isotopic composition between the SMOW and our sample is 0,0016 kg/m^3, as has been described in 2.1. We also used Kell's equation of thermal expansion to calculate values for $\varrho(t_{ref})$. The relative uncertainty in ϱ_{max} used here is believed to be of the order of 1×10^{-6}, and the resulting uncertainty in the density ratio should be less than 0,1 ppm. The choice of the thermal expansion equation also has little effect on the final values of $\varrho(t)/\varrho_{max}$, since t_{ref} is close to 4 °C.

3. Results

A total of 79 pairs of temperature and density ratio $\varrho(t)/\varrho_{max}$ values was obtained from 4 series of measurements. They are listed in Table 2.

Out of the 79 measurement points, 72 were fitted to a functional form proposed by Thiesen [14], and the following function was obtained.

$$\varrho(t)/\varrho_{max} = 1 - \frac{(t-3{,}98152)^2\,(t+396{,}18534)\,(t+32{,}28853)}{609\,628{,}6\,(t+83{,}12333)\,(t+30{,}24455)}\,. \qquad (4)$$

Table 2. Measurements of temperature and $\varrho(t)/\varrho_{max}$. The δ's are the residuals from (4)

No.	t/°C	$\varrho(t)/\varrho_{max}$	δ/ppm	No.	t/°C	$\varrho(t)/\varrho_{max}$	δ/ppm	No.	t/°C	$\varrho(t)/\varrho_{max}$	δ/ppm	No.	t/°C	$\varrho(t)/\varrho_{max}$	δ/ppm
Series 1				Series 2				Series 3				Series 4			
1	0,7051	0,9999115	0,3	1	0,7048	0,9999110	−0,1	1	0,7055	0,9999114	0,2	1	0,7080	0,9999112	−0,1
2	2,1184	0,9999718	0,0	2	2,1162	0,9999716	−0,1	2	2,1235	0,9999717	−0,2	2	2,1253	0,9999718	−0,2
3	4,0773	0,9999999	0,0	3	4,0753	0,9999999	0,0	3	4,0798	0,9999999	0,0	3	4,0846	0,9999999	0,0
4	6,0963	0,9999651	0,0	4	6,0963	0,9999652	0,1	4	6,0999	0,9999651	0,2	4	6,1047	0,9999649	0,2
5	8,1810	0,9998651	0,1	5	8,1803	0,9998652	0,1	5	8,1840	0,9998649	0,0	5	8,1900	0,9998648	0,3
6	10,1159	0,9997173	−0,1	6	10,1175	0,9997173	0,1	6	10,1209	0,9997169	0,0	6	10,1282	0,9997165	0,2
7	15,0551	0,9991195	0,1	7	15,0550	0,9991195	0,0	7	15,0604	0,9991186	−0,1	7	15,0694	0,9991173	0,0
8	20,1116	0,9982090	−0,2	8	20,1132	0,9982087	−0,1	8	20,1167	0,9982079	−0,2	8	20,1267	0,9982060	0,0
9	25,0752	0,9970532	−0,2	9	25,0771	0,9970531	0,2	9	25,0781	0,9970524	−0,2	9	25,0937	0,9970485	−0,1
10	30,1455	09956302	−0,2	10	30,1476	0,9956301	0,2	10	30,1485	0,9956295	−0,1	10	30,1659	0,9956242	−0,1
11	35,0860	0,9940291	0,2	11	35,0883	0,9940286	0,6	11	35,0894	0,9940276	−0,1	11	35,1076	0,9940213	−0,1
12	40,0698	0,9922148	−0,1	12	40,0712	0,9922146	0,3	12	40,0722	0,9922139	0,0	12	40,0915	0,9922065	0,0
13	45,1605	0,9901714	0,4	13	45,1661	0,9901689	0,2	13	45,1628	0,9901700	0,0	13	45,1832	0,9901613	−0,2
14	55,1678	0,9856374	0,0	14	55,1700	0,9856365	0,2	14	49,8670	0,9881203	−0,3	14	51,8866	0,9871957	0,0
15	64,9600	0,9805982	0,1	15	65,1614	0,9804887	0,1	15	55,1687	0,9856367	−0,2	15	62,0182	0,9821707	−0,5
16	74,3591	0,9752501	0,1	16	74,6080	0,9751021	0,2	16	59,8964	0,9832746	−0,1	16	72,5138	0,9763377	0,1
17	85,6222	0,9682324	−0,1	17	85,6314	0,9682265	0,0	17	65,1572	0,9804905	−0,4	17	85,6564	0,9682103	0,1
18*	35,1004	0,9940238	−0,1	18*	35,0967	0,9940250	−0,1	18	69,6167	0,9780085	0,0	18*	35,1072	0,9940203	−1,3
				19*	10,1142	0,9997175	−0,1	19	74,6047	0,9751039	0,0	19*	10,1247	0,9997152	−1,4
								20	79,7404	0,9719774	0,3				
								21	85,6323	0,9682255	−0,4				
								22*	35,0939	0,9940249	−1,2				
								23*	25,0851	0,9970497	−1,1				

* Data taken for reproducibility check, not used in the least squares fittings

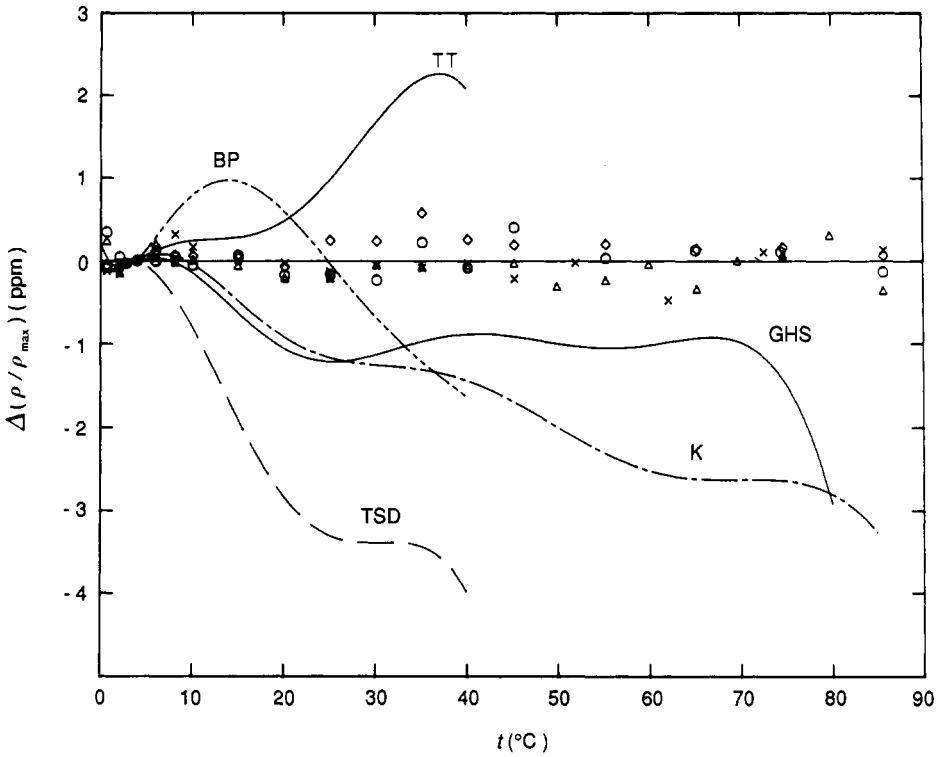

Fig. 4. Residuals of observed values and comparison with literature values. Base line is (4). ○: series 1, ◇: series 2, △: series 3, ×: series 4. TT: Tilton and Taylor [15]. This is based on Chappuis' measurement [1]. The temperature scale used is assumed to be equivalent to the IPTS-68 [4]. K: Kell [16]. This is basically an extension of the Tilton and Taylor equation to higher temperatures. The temperature scale used by Chappuis is assumed to be equivalent to the IPTS-48 [5]. GHS: Gildseth, Habenschuss and Spedding [17]. This is based on the Tilton and Taylor equation at temperatures less than 40 °C. The temperature scale used is the IPTS-48. TSD: Thiesen, Scheel and Diesselhorst [2]. The temperature scale used is assumed to be equivalent to the IPTS-68 [4]. BP: Bell and Patterson [18]

Table 3. Sources of errors in $\varrho(t)/\varrho_{max}$

Source of error	Amount	Uncertainty in $\varrho(t)/\varrho_{max}$ (ppm)		
		at 20 °C	40 °C	85 °C
(Thermal expansion of water)				
Mass of sample water	1 mg	0,01	0,01	0,17
Density of water at reference temperature	< 3 ppm	< 0,01	< 0,01	< 0,1
Volume of dilatometer	1 mm^3	0,03	0,07	0,15
Calibration of balance for mercury in bottle	0,1 mg	0,07	0,07	0,07
Density of mercury in dilatometer	1–5 ppm	0,04	0,1	0,1
Mean temperature of the part of capillary with temperature gradient	3 K	0,3	0,3	0,3
Calibration of Pt resistance thermometer	0–0,3 mK	0,02	0,08	0,2
Temperature distribution in thermostat	0,2–1 mK	0,04	0,12	0,65
Instability of dilatometer volume	$0{,}7\times\lvert(t/°C)-4\rvert/81$ (ppm)	0,2	0,37	0,7
(Thermal expansion of water cell)				
Wavelength stability of laser	$<3\times10^{-8}$	< 0,1	< 0,1	< 0,1
Initial length of the cell	0,1 mm	0,03	0,05	0,1
Misalignment of cell axis	2×10^{-4} rad	0,05	0,05	0,05
Residual gas pressure	4 Pa	0,03	0,03	0,03
Cell temperature	0–0,2 K	0,0	0,1	0,3
Type A error [19]		0,2	0,2	0,2
Choice of fitting function		0,2	0,2	0,2
Total error (Root of sum squares)		0,5	0,6	1,1

The standard deviation of a single measurement as calculated from the residuals is 0,2 ppm. The remaining seven points marked with asterisks in Table 2 were taken to check overall reproducibility, and were not used for the fitting. The information they carry has been taken into account in assigning uncertainties, as will be described in the next section. Two other types of functions, a polynomial of the eighth order and a Kell-type function, were also used for fitting (Appendix). It was found that the differences among the values these equations give are less than 0,2 ppm for the most part. Accordingly, it would be appropriate to assume that the bias introduced by an arbitrary choice of functional form is less than 0,2 ppm.

4. Discussion

The sources of errors in the density ratio $\varrho(t)/\varrho_{max}$ are listed in Table 3. The following are comments on how the uncertainties have been estimated.

A small systematic bias in pressure measurement has no effect on the density ratio as long as the bias remains the same throughout a series; hence, the systematic error in pressure measurement is not included in the table. The positions of maxima of fringes in the Fizeau interferometer shift when the reflectivities of the mirrors are high and the distance between the mirrors is large, which is the case with our interferometer. This shift, however, does not affect the result if the quantity to be measured is displacement; hence, it is not included in the table. The temperature distribution along the cell during interferometric measurement was 0,2 K at the highest temperature. The error in the mean temperature of the cell is thus estimated to be less than 0,2 K, which corresponds to 0,3 ppm of uncertainty in $\varrho(t)/\varrho_{max}$.

At the end of each run, in which the temperature was raised stepwise from 0 °C to 85 °C, the temperature was lowered to the room temperature in order to check the overall reproducibility. The shifts observed are about 1 ppm or less in terms of $\varrho(t)/\varrho_{max}$ as shown in Table 2, and they appear to have resulted from a slight deformation of the grease layers during the measurement cycles. In order to check this effect further, the dilatometer was subjected to five cycles of temperature changes to and from 4 °C and 85 °C, and the overall volume changes on going from 4 °C to 85 °C and vice versa were measured. All points were observed to fall within $\pm 0{,}7$ ppm with a standard deviation of 0,4 ppm. Accordingly, we took into account this effect in our error budget assuming that the uncertainty is given by the following formula:

$$\delta\,\varrho = 0{,}7 \times 10^{-6}\{[(t/°C) - 4]/81\}.$$

This is because the measurement at t_{ref}, which is close to 4 °C, is taken as the reference of calculation. The uncertainty from this cause should be zero at this temperature, and should increase as one moves away from this temperature to reach eventually 0,7 ppm at 85 °C.

Figure 4 shows the residuals of the observed values when they are fitted to (4). It also shows the deviations from (4) of five formulae taken from the existing literature. The values included are those of Tilton and Taylor [15], Kell [16], Thiesen, Scheel and Diesselhorst [2], Gildseth, Habenschuss and Spedding [17], and Bell and Patterson [18].

Appendix: Fittings to Other Functional Forms

If the data are fitted to one of the rational functions of the form proposed by Kell [16],

$$\varrho(t)/\varrho_{max} = (A_0 + \Sigma A_i t^{2i-1})/(1 + \Sigma B_j t^{2j}) \quad (i = 1,4 : j = 1,4) \tag{5}$$

$A_0 = 9{,}9986784 \times 10^{-1}$, $A_1 = 6{,}7826308 \times 10^{-5}$,
$A_2 = 1{,}0365704 \times 10^{-7}$, $A_3 = 1{,}7485485 \times 10^{-11}$,
$A_4 = 8{,}4152542 \times 10^{-16}$,
$B_1 = 9{,}0887089 \times 10^{-6}$, $B_2 = 1{,}4974442 \times 10^{-9}$,
$B_3 = 1{,}6006519 \times 10^{-13}$, $B_4 = 2{,}8106977 \times 10^{-18}$,

the standard deviation of fitting is 0,2 ppm.

If a polynomial of the eighth order,

$$\varrho(t)/\varrho_{max} = \Sigma A_i t^{i-1} \quad (i = 1,9) \tag{6}$$

$A_1 = 9{,}9986785 \times 10^{-1}$, $A_2 = 6{,}7819907 \times 10^{-5}$,
$A_3 = -9{,}0858952 \times 10^{-6}$, $A_4 = 1{,}0288239 \times 10^{-7}$,
$A_5 = -1{,}4077910 \times 10^{-9}$, $A_6 = 1{,}6355966 \times 10^{-11}$,
$A_7 = -1{,}3688193 \times 10^{-13}$, $A_8 = 6{,}9699179 \times 10^{-16}$,
$A_9 = -1{,}5914816 \times 10^{-18}$,

is used, the standard deviation is 0,2 ppm.

References

1. P. Chappuis: Trav. Mem. Bur. Intern. Poids et Mesures **13,** D1–D40 (1907)
2. M. Thiesen, K. Scheel and H. Diesselhorst: Phys. Tech. Reichs. Wiss. Abhandl. **3,** 1–70 (1900)
3. C. E. Guillaume: Trav. Mem. Bur. Intern. Poids et Mesures **14,** (1910); P. Chappuis: Trav. Mem. Bur. Intern. Poids et Mesures **14,** (1910); J. Mace de Lepnay, J. H. Buisson and J. R. Benoit: Trav. Mem. Bur. Intern. Poids et Mesures **14,** (1910)
4. M. Menache and G. Girard: Metrologia **9,** 62–68 (1973)
5. G. S. Kell: J. Chem. Eng. Data **20,** 97–105 (1975)
6. IUPAC Commission I. 4. Recommendation for the Redetermination of the Absolute Density of Water, 1974
7. R. Masui, S. Seino, O. Senda and Y. Okamoto: *Proc. the 10th Int. Conf. the Properties of Steam* (Moscow) **1,** 158–166 (1986)
8. N. Bignell: Metrologia **19,** 57–59 (1983)
9. Formule pour la détermination de la masse volumique de l'air humide: BIPM Rapport 81/8, pp. 19
10. K. E. Bett, P. F. Hayes and D. M. Newitt: Phil. Trans. Roy. Soc. **247 A,** 59–100 (1954)
11. H. Preston-Thomas: Metrologia **27,** 3–10 (1990)
12. A. H. Cook: Brit. J. Appl. Phys. **7,** 285–293 (1956)
13. P. H. Bigg: Brit. J. Appl. Phys. **15,** 1111–1113 (1964)
14. M. Thiesen: Phys. Tech. Reichs. Wiss. Abhandl. **4,** 1–32 (1904)
15. L. W. Tilton and J. K. Taylor: J. Res. Nat. Bur. Stand. **18,** 205–214 (1937)
16. G. S. Kell: J. Phys. Chem. Ref. Data **6,** 1109–1131 (1977)
17. W. Gildseth, A. Habenschuss and F. H. Spedding: J. Chem. Eng. Data **17,** 402–409 (1972)
18. G. A. Bell and J. B. Patterson: *Precision Measurement and Fundamental Constants II,* B. N. Taylor and W. D. Phillips (eds.), Natl. Bur. Stand. (U.S.), Spec. Publ. 617, (U.S. Government Printing Office, Washington D.C. 1984) pp. 445–447
19. P. Giacomo: Metrologia **17,** 69–74 (1981)